Plasmons in a free-standing nanorod with a two-dimensional parabolic quantum well caused by surface states*

Song Ya-Feng(宋亚峰)[a], Lü Yan-Wu(吕燕伍)[b], Wen Wei(文 伟)[c], Liu Xiang-Lin(刘祥林)[a], Yang Shao-Yan(杨少延)[a], Zhu Qin-Sheng(朱勤生)[a]†, and Wang Zhan-Guo(王占国)[a]

[a] *Key Laboratory of Semiconductor Materials Science, Institute of Semiconductors, Chinese Academy of Sciences, Beijing* 100083, *China*

[b] *Department of Physics, Beijing Jiaotong University, Beijing* 100044, *China*

[c] *State Key Laboratory for Superlattices and Microstructures, Institute of Semiconductors, Chinese Academy of Sciences, Beijing* 100083, *China*

(Received 18 October 2011; revised manuscript received 15 November 2011)

The collective charge density excitations in a free-standing nanorod with a two-dimensional parabolic quantum well are investigated within the framework of Bohm–Pine's random-phase approximation in the two-subband model. The new simplified analytical expressions of the Coulomb interaction matrix elements and dielectric functions are derived and numerically discussed. In addition, the electron density and temperature dependences of dispersion features are also investigated. We find that in the two-dimensional parabolic quantum well, the intrasubband upper branch is coupled with the intersubband mode, which is quite different from other quasi-one-dimensional systems like a cylindrical quantum wire with an infinite rectangular potential. In addition, we also find that higher temperature results in the intersubband mode (with an energy of 12 meV ($\sim$ 3 THz)) becoming totally damped, which agrees well with the experimental results of Raman scattering in the literature. These interesting properties may provide useful references to the design of free-standing nanorod based devices.

Keywords: plasmons, two-dimensional parabolic quantum well, terahertz nanodevices, nanorod

PACS: 73.20.Mf, 73.21.Hb **DOI:** 10.1088/1674-1056/21/5/057302

1. Introduction

Collective excitations (plasmons) in low-dimensional electron systems have attracted much attention. Many remarkable achievements have been obtained for plasmons[1−10] and surface plasmons[11,12] experimentally[1−5] and theoretically,[6−10] especially for the great potential applications.[13,14] Among them, a quasi-one-dimensional (Q1D) system is one of the research focuses due to its interesting properties[15,16] and many promising potential applications in semiconductor devices,[17] especially terahertz devices.[18−20] The one-dimensional (1D) parabolic potential model has been extensively used for many Q1D systems such as quantum wires (QWs) and quantum well wires (QWWs). For example, Borges *et al.*[9] calculated the collective excitations in QWs for two and three subbands by using the 1D parabolic quantum well model. Bratschitsch *et al.*[18] observed terahertz emission corresponding to the intersubband plasmon of the parabolic quantum well. In most of the Q1D systems,[8−11] the 1D parabolic quantum well model was used by assuming a zero-thickness plane approximation, which is reasonable when the confinement in one dimension is much stronger than the other for a QW or QWW.[9]

There is another kind of Q1D structure, the free-standing semiconductor nanorod,[21−23] which is usually used as a kind of promising and interesting structure in nanodevices.[24,25] However, to our knowledge, neither collective particle excitation characteristics nor single particle excitation characteristics in a free-standing nanorod have been investigated. The potential quantum confinement in a free-stanting nanorod is different from those in QWs and QWWs. Generally, the wells in QWs and QWWs are formed by the

*Project supported by the National Natural Science Foundation of China (Grant Nos. 60976008, 61006004, 61076001, and 10979507), the National Basic Research Program of China (Grant No. A000091109-05), and the National High Technology Research and Development Program of China (Grant No. 2011AA03A101).

†Corresponding author. E-mail: qszhu@semi.ac.cn

© 2012 Chinese Physical Society and IOP Publishing Ltd

band offset; while in a free-standing nanorod, other factors (such as surface states) usually make the case different. Due to the existence of surface states,[26,27] which is caused by dangling bonds and surface atom reconstruction, etc., in a nanorod, no matter what they catch or arrest (holes, electrons, atoms or even nothing), they are usually charged when exposed to air. Subsequently, it will cause the conduction band and the valence band to bend along the radial direction, and a surrounding depletion region subsequently forms. In this case, the two-dimensional (2D) parabolic potential (instead of the 1D parabolic potential model for QWWs) becomes a reasonable simplified model for the surrounding depletion region to investigate the excitations of electrons in the nanorod.

In this paper, we investigate the collective charge density excitations in the free-standing nanorod caused by surface states in an isotropic 2D parabolic potential regime, and discuss the potential applications in a terahertz nanodevice. The electron density and temperature dependences of dispersion features are also investigated. The rest of the present paper is organized as follows. In Section 2, we describe the theoretical model. In Section 3, we present the numerical results and discussion, including the comparison with the cylindrical quantum wire with infinite rectangular potential and the potential applications in terahertz nanodevices. Finally, in Section 4, we present the conclusions.

2. Theoretical model

2.1. Wave functions in a two-dimesional parabolic-well nanorod

The real environment of the free-standing nanorod is much more complicated.[21–23] In this case, the two-dimesional parabolic quantum well model is a reasonable simplification for a free-standing nanorod caused by surface states (see Appendix A). The behaviours of the electrons in a two-dimesional parabolic-well nanorod (2D-PWR) Q1D system can be described by the effective-mass Schrödinger equation with the Hamiltonian in the cylindrical coordinates

$$H(\rho,\theta) = -\frac{\hbar^2}{2m^*}\Big(\frac{\partial^2}{\partial\rho^2}+\frac{1}{\rho}\frac{\partial}{\partial\rho}+\frac{1}{\rho^2}\frac{\partial^2}{\partial\theta^2}\Big) + \frac{1}{2}m^*\Omega^2\rho^2, \tag{1}$$

where $\Omega = \sqrt{e^2N_{\rm D}^+/m^*\varepsilon_{\rm s}}$. By solving this cylindrically symmetrical Hamiltonian in the Schrödinger equation, we obtain the wave function with the following expression:[28]

$$\psi(\boldsymbol{X}) \equiv \psi_{nm}(\rho,\theta) = C_{nm}\rho^{|m|}F(-n,|m|+1,\alpha^2\rho^2)\,{\rm e}^{-\alpha^2\rho^2/2}\,{\rm e}^{{\rm i}\,m\theta}, \tag{2}$$

where $\alpha^2 = \sqrt{e^2N_{\rm D}^+m^*/\varepsilon_{\rm s}\hbar^2}$, C_{nm} is the normalization factor, and $F(\alpha,\beta,\gamma)$ is the confluent hypergeometric function. The corresponding energy of the whole quantum system is

$$E_{nmk_z} = \frac{\hbar^2k_z^2}{2m^*} + (2n+|m|+1)\hbar\omega_0, \tag{3}$$

with $\omega_0 = \Omega$.

Specifically, we have the eigenstates of the lowest two subbands

$$\begin{cases} \psi_1(\boldsymbol{X}) \equiv \psi_{00}(\rho,\theta) = \frac{\alpha}{\sqrt{\pi}}\,{\rm e}^{-\alpha^2\rho^2/2}, \\ \psi_2(\boldsymbol{X}) \equiv \psi_{01}(\rho,\theta) = \frac{\alpha^2}{\sqrt{\pi}}\rho\,{\rm e}^{-\alpha^2\rho^2/2}\,{\rm e}^{{\rm i}\,\theta}, \end{cases} \tag{4}$$

and the eigen energy $E_1 \equiv E_{00} = \hbar\omega_0$ and $E_2 \equiv E_{01} = E_{0(-1)} = 2\hbar\omega_0$. For the 2D-PWR system, the second subband is degenerate with $m = \pm1$. For the rest of this paper, for simplification, we only consider the second subband of $m = 1$ (the case of $m = -1$ is quite similar).

Moreover, the schematic diagram of 2D parabolic quantum well confined potential for the free-standing nanorod caused by surface states is shown in Fig. 1. The wave functions and eigen energies of the ground and the first excited subbands are also shown (Si is doped at $N_{\rm D} = 2\times10^{17}$ cm^{-3}. The other material constants are those of GaAs). The energy separation between the two lowest subbands is 12.5 meV, corresponding to 3.0 THz.

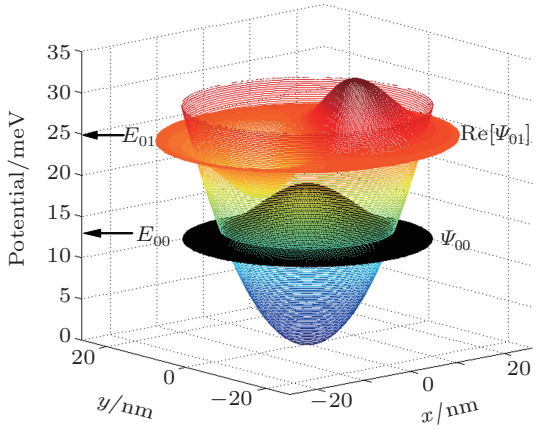


Fig. 1. (colour online) Schematic diagram of the 2D parabolic quantum well model for the free-standing nanorod caused by surface states. The wave functions and eigen energies of the ground and the first excited subbands are also shown. The energy separation between the two lowest subbands is 12.5 meV (∼3.0 THz).

2.2. Analytical expressions of the Coulomb matrix and semi-analytical approximation for dispersion

For many cases,[6,7] Bohm–Pine's random-phase approximation (RPA) is a reasonable approximation for plasmon studies. The collective excitation spectrum of this cylindrical system is determined by searching the zeros of dielectric function determination. Therefore, we use the standard linear-response theory within the framework of RPA to study the collective excitations of 2D-PWR. It is found experimentally[29] that the coupling between electrons and phonons is important for polar semiconductors, especially when the plasmon energy is close to the longitudinal optical (LO) phonon energy (36 meV for GaAs). However, for a GaAs nanorod, the plasmon energy is significantly smaller than 36 meV and it is a reasonable approximation for us to ignore this coupling. To be a good approximation, we ignore the effects of exchange correlations, image effects and the coupling with phonons. The dielectric function matrix elements for our 2D-PWR Q1D system then read

$$\varepsilon_{ijkl}(q_z,\omega)=\delta_{il}\delta_{jk}-V_{ijkl}(q_z)\Pi_{kl}(q_z,\omega), \quad (5)$$

where

$$\Pi_{kl}(q_z,\omega)=2\int\frac{\mathrm{d}k_z}{2\pi}\frac{f_0\left[\dfrac{\hbar^2\left(k_z+q_z\right)^2}{2m^*}+E_k\right]-f_0\left[\dfrac{\hbar^2k_z^2}{2m^*}+E_l\right]}{\dfrac{\hbar^2\left(k_z+q_z\right)^2}{2m^*}+E_k-\dfrac{\hbar^2k_z^2}{2m^*}-E_l+\hbar\omega^+}, \ (k,l=1,2), \quad (6)$$

and $V_{ijkl}(q_z)$ is the electron–electron Coulomb interaction matrix element as shown in Appendix B.

Then we derive the new expression of Coulomb matrix elements in the relative coordinates and centroid coordinates as

$$\widetilde{V}_{ijkl}(q_z)=\frac{2e^2}{\varepsilon_{\mathrm{L}}}\times 4\int_0^{2\pi}\mathrm{d}\phi\int_0^{\infty}\Big[\int_0^{2\pi}\mathrm{d}\phi'\int_0^{\infty}\Phi_i(t,\phi,t',\phi')\times\Phi_j^*(t,\phi,t',\phi')\Phi_k(t,\phi,t',\phi')\Phi_l^*(t,\phi,t',\phi')K_0(2q_zt')t'\,\mathrm{d}t'\Big]t\,\mathrm{d}t, \quad (7)$$

where $\Phi_i(t,\phi,t',\phi')$, $\Phi_j^*(t,\phi,t',\phi')$, $\Phi_k(t,\phi,t',\phi')$, $\Phi_l^*(t,\phi,t',\phi')$ are the new wave functions in the relative coordinates and centroid coordinates with $\boldsymbol{Y}=(\boldsymbol{X}+\boldsymbol{X}')/2$, $\boldsymbol{Y}'=(\boldsymbol{X}-\boldsymbol{X}')/2$ and $\boldsymbol{X}\equiv(r,\theta)$, $\boldsymbol{X}'\equiv(r',\theta')$, $\boldsymbol{Y}\equiv(t,\phi)$, $\boldsymbol{Y}'\equiv(t',\phi')$ are the old and new coordinates in polar forms respectively. Note that the complicated expressions in the zero order of the modified Bessel function $K_0(\sqrt{|u'^2-2uu'\cos(\theta-\theta')+u^2|})$ (Eq. (B1d)) are replaced by the simple form with single variable $K_0(2q_zt')$, which is very meaningful for analytical simplification and numerical calculations.

Specifically, we find that the first three Coulomb matrix elements have very simple forms with only singlet integrals as follows:

$$\widetilde{V}_{1111}(q_z)=\frac{2e^2}{\varepsilon_{\mathrm{L}}}\beta^2\int_0^{\infty}t\,\mathrm{e}^{-\frac{\beta^2}{2}t^2}K_0(t)\,\mathrm{d}t, \quad (8a)$$

$$\widetilde{V}_{2222}(q_z)=\frac{2e^2}{\varepsilon_{\mathrm{L}}}\frac{\beta^2}{2}\int_0^{\infty}t\Big(1+\frac{\beta^4}{8}t^4\Big)\,\mathrm{e}^{-\frac{\beta^2}{2}t^2}K_0(t)\,\mathrm{d}t, \quad (8b)$$

$$\widetilde{V}_{1122}(q_z)=\frac{2e^2}{\varepsilon_{\mathrm{L}}}\frac{\beta^2}{2}\int_0^{\infty}t\Big(1+\frac{\beta^2}{2}t^2\Big)\,\mathrm{e}^{-\frac{\beta^2}{2}t^2}K_0(t)\,\mathrm{d}t. \quad (8c)$$

These simplifications greatly reduce the amount of computation time reqired to obtain numerical results.

Figure 2(a) shows the wave vector dependence of the seven independent Coulomb matrix elements $V_{ijkl}(q_z)$ in the logarithmic coordinate. Figure 2(b) shows the comparison of the original expressions Eqs. (B1a)–(B1c) and the simplified ones (Eqs. (8a)–(8c)) for the numerical results of Coulomb matrix elements V_{1111}, V_{1122}, and V_{2222} in the logarithmic coordinate. It is clear to see that these simplified analytical expressions (Eqs. (8)) match very well with the original ones for most wave vectors, indicating that they are very accurate substitutions of Eqs. (B1).

In addition, from Fig. 2(a) we can safely take $V_{1212}(q_z)$, $V_{1112}(q_z)$ and $V_{1222}(q_z)$ to be zero. Particularly, when the second subband is almost unoccupied, we have $\Pi_{22}(q_z,\omega)\approx 0$, so dielectric function in two-subband model can be simplified further into

$$1-V_{1111}(q_z)\Pi_{11}(q_z,\omega)=0, \quad (9a)$$

$$1-|V_{1221}(q_z)|^2\,\Pi_{21}(q_z,\omega)\Pi_{12}(q_z,\omega)=0. \quad (9b)$$

Equation (9a) indicates that the one-subband approximation is part of this semi-analytical simplification. In this case, the dielectric function then reads

$$\det|\varepsilon_{ijkl}(q_z,\omega)|\approx\varepsilon_{1111}$$

$$
\begin{aligned}
&= 1 - V_{1111}(q_z)\Pi_{11}(q_z,\omega) \\
&= 1 - \frac{2e^2}{\varepsilon_{\rm L}}\frac{\beta^4}{\pi^2}\int_0^{2\pi}{\rm d}\theta\int_0^{\infty} u\,{\rm e}^{-\beta^2u^2} \\
&\quad\times\Big[\int_0^{2\pi}{\rm d}\theta'\int_0^{\infty} u'\,{\rm e}^{-\beta^2u'^2}K_0 \\
&\quad\times(\sqrt{|u'^2-2uu'\cos(\theta-\theta')+u^2|}){\rm d}u'\Big]{\rm d}u \\
&\quad\times\Pi_{11}(q_z,\omega). \qquad (10)
\end{aligned}
$$

However, after using the new simplified expression of Coulomb matrix elements given by Eq. (8), it becomes a much simpler expression like

$$
\begin{aligned}
&\det|\varepsilon_{ijkl}(q_z,\omega)| \\
&\approx \widetilde{\varepsilon}_{1111} \\
&= 1 - \widetilde{V}_{1111}(q_z)\Pi_{11}(q_z,\omega) \\
&= 1 - \frac{2e^2}{\varepsilon_{\rm L}}\beta^2\int_0^{\infty} t\,{\rm e}^{-\frac{\beta^2}{2}t^2}K_0(t)\,{\rm d}t\Pi_{11}(q_z,\omega). \qquad (11)
\end{aligned}
$$

Later the inset in Fig. 3 shows the comparisons between dispersion spectrum results obtained from Eqs. (5), (10) and (11). It also shows a dispersion relation with good accuracy for certain cases.

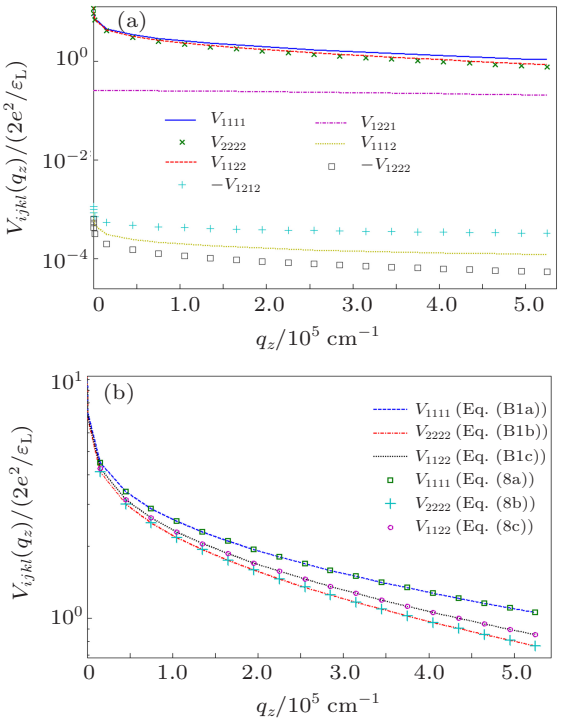


Fig. 2. (colour online) (a) Wave vector dependences of the Coulomb matrix elements $V_{ijkl}(q_z)$. (b) Comparison of the original expressions Eqs. (B1a)–(B1c) (lines) with the simplified ones Eqs. (8a)–(8c) (crosses, squares and circles) for the numerical results of Coulomb matrix elements V_{1111}, V_{1122} and V_{2222}. All are in the logarithmic coordinate.

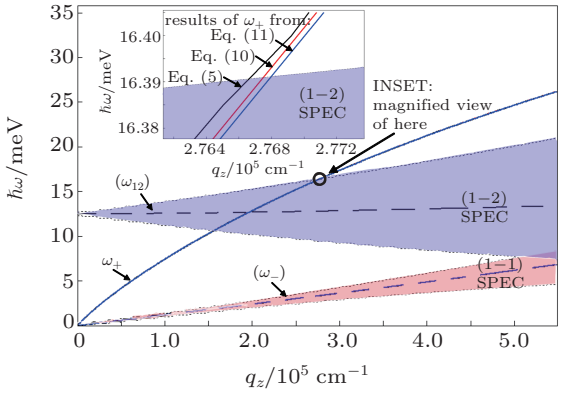


Fig. 3. (colour online) Dispersion relations of electrons in a 2D parabolic quantum well nanorod (2D-PWR) system (one subband occupied case). The three shaded areas represent the (1–2) and (1–1) single particle excitation continua (SPEC), respectively. The broken lines represent the Landau damped collective modes and ω_- and ω_{12} in brackets mean that they are damped. $T = 1.75$ K and $E_{\rm F} = E_1 + 0.5\Delta E_{21} = 1.5E_1$ ($\Delta E_{21} \equiv E_2 - E_1$). The inset shows the comparison between dispersion spectrum results obtained in the different approximations from Eqs. (5), (10), and (11). The other constants of material are the same as those in Fig. 1.

3. Results and discussion

The dispersion relations of electrons in the 2D-PWR system with the lowest subband occupied are plotted in Fig. 3, where we take $E_{\rm F} = E_1 + 0.5\Delta E_{21} = 1.5E_1$ ($\Delta E_{21} \equiv E_2 - E_1$), $\gamma = 5 \times 10^{-4}$ meV and $T = 1.75$ K. The other material constants are the same as those in Fig. 1. The figure shows that the upper branch ω_+ is always undamped with a large energy but the lower branch and the intersubband mode is always damped, which is different from those in other Q1D systems. For example, in cylindrical-shaped quantum wire with an infinite rectangular potential, the upper branch ω_+ has a much lower energy and is well separated with the intersubband excitation mode.[30] This may be due to the fact that in the 2D parabolic well, the overlapping of the wave functions is expected to be not so significant as that in the infinite rectangular cylindrical quantum well, so the Coulomb matrix elements are different from those of the later system. This affects the results of Eq. (5) and finally this discrepancy.

Moreover, the inset in Fig. 3 shows the magnified comparisons of the ω_+ modes from Eqs. (5) , (10), and (11) with the lowest subband occupied. We can see that the three results match with each other very well, indicating that our simplified expressions are reasonably approximate expressions.

As shown in Fig. 4, the two-subband occupied case becomes a more complicated case in which the populations on the subbands are much higher than the above. In this case, the intrasubband ω_- mode and intersubband ω_{12} mode both become undamped as the (1–2) intersubband SPEC splits and the new SPEC: (2–2) intrasubband SPEC emerges. Meanwhile, the intrasubband ω_+ mode becomes coupled with the intersubband mode and becomes broken modes near the crossover point. These characteristics are quite different from those of other quasi-1D systems like cylindrical quantum wire with infinite rectangular potential,[30] because in the latter system, the intrasubband upper mode is usually uncoupled with the intersubband mode even for larger wave vectors.

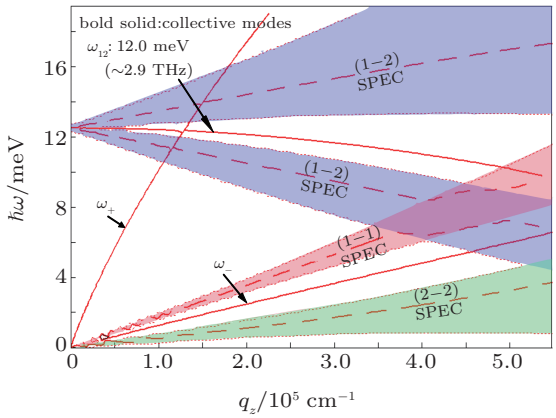


Fig. 4. (colour online) Dispersion relations of electrons in the 2D-PWR system (two subbands occupied case). The broken lines represent the Landau damped collective modes. The shaded areas represent the (1–2), (1–1) and (2–2) SPEC, respectively. Note that the (1–2) SPEC splits into two parts. The basic parameters are the same as those in Fig. 3 except for $E_{\rm F} = E_2 + 0.1\Delta E_{21} = 2.1E_1$. The intersubband absorption peak of the incident light is at 3 THz. By changing the Fermi level, we may control the "on" or "off" of the terahertz absorption.

It is also noteworthy that when two subbands are occupied, the small negative dispersion of the undamped intersubband mode indicates that the resonant energy is a little bit smaller than the energy separation of the lowest two subbands. This means that the absorption peak of Raman scattering is at 3 THz. Thus, one might expect that the free-standing nanorod is suitable for the fabrication of nanodevices working in the terahertz range. By changing the Fermi level, we may control the "on" or "off" of the terahertz absorption.

The influences of electron densities with different occupation levels on dispersion characteristics of 2D-PWR are plotted in Fig. 5. Only the lowest subbands are occupied each with the one-dimensional electron density of $n_{\rm 1D}^{(1)}(E_{\rm F1}) = 2.962 \times 10^5$ cm^{-1}, and $n_{\rm 1D}^{(1)}(E_{\rm F2}) = 8.944 \times 10^5$ cm^{-1} respectively. Here, the one-dimensional electron density of the i-th subband in the nanorod is calculated by[31]

$$n_{\rm 1D}^{(i)}(E_{\rm F}) = \sqrt{\frac{2m^* k_{\rm B}T}{\pi^2\hbar^2}} F_{-1/2}\Big(\frac{E_{\rm F} - E_i}{k_{\rm B}T}\Big), \qquad (12)$$

where $F_{-1/2}$ is the Fermi–Dirac integral. It shows that for the intrasubband ω_+ mode, the higher the electron density is, the higher the energies of the intrasubband plasmon and single-particle excitations are, and the larger the intersubband SPEC is.

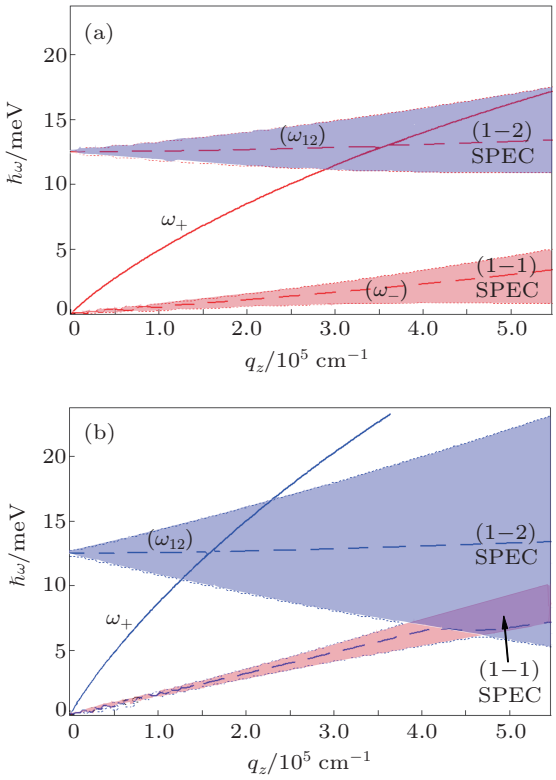


Fig. 5. (colour online) Dispersion relations of electrons in the 2D-PWR system for different electron densities with different occupation levels ($T = 1.75$ K): (a) $E_{\rm F1} = E_1 + 0.1\Delta E_{21} = 1.1E_1$, (b) $E_{\rm F2} = E_1 + 0.9\Delta E_{21} = 1.9E_1$.

In addition, we also investigate the temperature dependence of plasmon dispersions of 2D-PWR system as shown in Fig. 6. It shows a slight increase in the intrasubband mode energy as temperature increases, in agreement with the results of Hubband model for GaAs-based Q1D electron gas by Vazifehshenas.[32] However, Vazifehshenas did not show the case of an intersubband mode. Figure 6 shows the interesting feature that for the free-standing nanorod, when the temperature is higher than a certain critical value

(about 10 K in this case), the connecting of the two (1–2) intersubband SPEC results in a total damping of the intersubband mode. This may be because the higher temperature increases the chance of electron–hole excitations via changing the Fermi distributions. Then it enlarges the energy region of the single particle excitation and makes the intersubband mode totally damped.

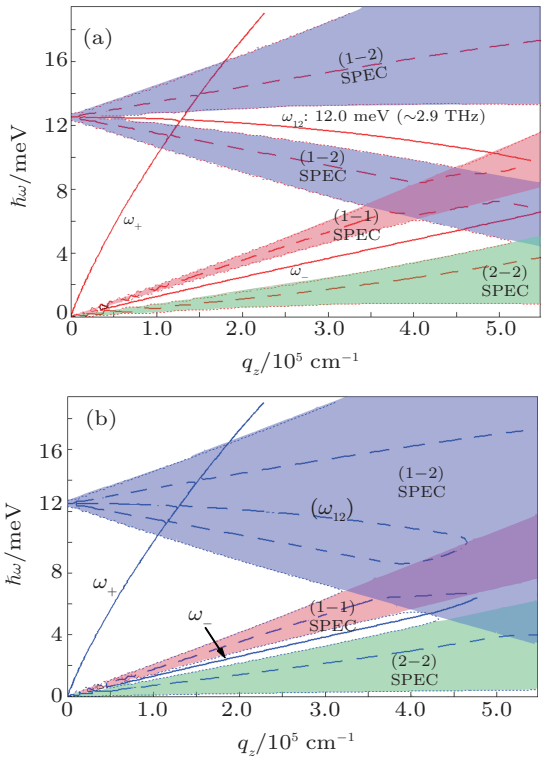


Fig. 6. (colour online) Dispersion relations of electrons in the 2D-PWR system with two lowest subbands occupied at different temperatures: (a) $T = 1.75$ K, (b) $T = 10$ K. $E_F = E_2 + 0.1\Delta E_{21} = 2.1E_1$. Higher temperature results in the intersubband mode with an energy of 12 meV (~3 THz) becoming totally damped.

This temperature dependence of an intersubband plasmon accords well with the experimental results of Raman scattering in the low-dimensional semiconductor structures.[33,34] Figures 1(a) and 1(b) in Ref. [33] show their Raman spectra in Si-doped GaAs/AlAs multiple quantum well at various temperatures. They find that the intensity of the "plasmon-like" high-frequency I_+ peak decreases with temperature increasing from 200 K to 350 K. At 350 K, the peak almost disappears, indicating that it tends to be totally damped. This is in good agreement with our numerical result. The main difference is the value of the critical temperature: "about 350 K in Ref. [33]" versus "about 10 K in our present work". This is because the exact structure we used is quite different: "GaAs/AlAs quantum wells in Ref. [33]" versus "GaAs nanorod in our present work". However, they still reveal similar trends of temperature dependence of intersubband plasmon in low-dimensional semiconductors, which stem from the temperature characteristic of Fermi–Dirac distribution of electrons. These interesting properties may provide useful references to the design of free-standing nanorod based devices. As for this interesting property, it may provide a new method of designing temperature dependent terahertz nanodevices.

4. Conclusion

It is shown that the 2D parabolic quantum well model works as a simple but reasonable model to investigate the collective charge density excitations in a free-standing nanorod with surface states. We use the framework of random phase approximation in the two-subband model. There are three plasmon modes effected in our quantum system. When the first excited subband is occupied, the (1–2) SPEC splits into two parts, resulting in the intersubband mode ω_{12} being undamped with small negative dispersion. Besides, in 2D-PWR, the intrasubband upper branch is coupled with the intersubband mode, which is quite different from the cases of other quasi-1D systems like cylindrical quantum wire with an infinite rectangular potential. Moreover, higher electron density can result in the higher plasmon energy of intrasubband modes and enlarge the intersubband SPEC greatly. Finally, we find that higher temperature can significantly increase the chance of single particle excitations to make the corresponding collective mode damped; and higher temperature also results in the intersubband mode with an energy of 12 meV (~3 THz) becoming totally damped, which agrees well with the experimental results of Raman scattering in literatures. These interesting properties may provide useful references for the design of free-standing nanorod-based devices.

Appendix A

For the 2D-PWR system, as the carriers are free in the z direction (assume that the z direction is along the nanorod), apparently the total wave function of this system is $\Psi(\boldsymbol{X}, z) = \psi(\boldsymbol{X})\varphi_{k_z}(z)$ where $\boldsymbol{X} \equiv$

(r,θ) in the x–y plane and $\varphi_{k_z}(z) = \mathrm{e}^{\mathrm{i}\,k_z z}/\sqrt{L_z}$. The surface states are assumed to bring negative charge Q^- into the system. The fixed surface charge induces a surrounded depletion region in the nanorod with a diameter r in a range of $r_0 < r < R_0$. The bending of the conduction band bottom $E_{\mathrm{c}}(r)$ is described by

$$E_{\mathrm{c}}(r) = \begin{cases} \dfrac{e^2 N_{\mathrm{D}}^+}{2\varepsilon_{\mathrm{s}}}(r^2 - 2r_0^2 \ln\dfrac{r}{r_0} - r_0^2), & r_0 < r < R_0, \\ 0, \qquad r < r_0 \end{cases} \tag{A1}$$

where r is the position in the radial direction, e is the free electron charge, and ε_{s} is the dielectric constant of GaAs material (Here, $\varepsilon_{\mathrm{s}} = \varepsilon_{\mathrm{L}}$). We find that in the $r_0 << R_0$ limit, it is reasonable to make the approximation of a surrounded parabolic well with the simpler form

$$\widetilde{E}_{\mathrm{c}}(r,\theta) = \frac{e^2 N_{\mathrm{D}}^+}{2\varepsilon_{\mathrm{s}}} r^2. \tag{A2}$$

Thus, we have the expression of Ω in Eq. (1), i.e., $\Omega = \sqrt{e^2 N_{\mathrm{D}}^+/m^*\varepsilon_{\mathrm{s}}}$.

Appendix B

The first three elements of electron–electron Coulomb interaction matrix for the 2D-PWR system are

$$V_{1111}(q_z) = \frac{2e^2}{\varepsilon_{\mathrm{L}}}\frac{\beta^4}{\pi^2}\int_0^{2\pi}\mathrm{d}\theta\int_0^{\infty} u\,\mathrm{e}^{-\beta^2 u^2}\left[\int_0^{2\pi}\mathrm{d}\theta'\int_0^{\infty} u'\,\mathrm{e}^{-\beta^2 u'^2} g(u,u',\theta,\theta')\mathrm{d}u'\right]\mathrm{d}u, \tag{B1a}$$

$$V_{2222}(q_z) = \frac{2e^2}{\varepsilon_{\mathrm{L}}}\frac{\beta^8}{\pi^2}\int_0^{2\pi}\mathrm{d}\theta\int_0^{\infty} u^3\,\mathrm{e}^{-\beta^2 u^2}\left[\int_0^{2\pi}\mathrm{d}\theta'\int_0^{\infty} u'^3\,\mathrm{e}^{-\beta^2 u'^2} g(u,u',\theta,\theta')\mathrm{d}u'\right]\mathrm{d}u, \tag{B1b}$$

$$V_{1122}(q_z) = \frac{2e^2}{\varepsilon_{\mathrm{L}}}\frac{\beta^6}{\pi^2}\int_0^{2\pi}\mathrm{d}\theta\int_0^{\infty} u\,\mathrm{e}^{-\beta^2 u^2}\left[\int_0^{2\pi}\mathrm{d}\theta'\int_0^{\infty} u'^3\,\mathrm{e}^{-\beta^2 u'^2} g(u,u',\theta,\theta')\mathrm{d}u'\right]\mathrm{d}u, \tag{B1c}$$

with

$$g(u,u',\theta,\theta') \equiv K_0(\sqrt{|u'^2 - 2uu'\cos(\theta-\theta') + u^2|}), \tag{B1d}$$

where $u \equiv q_z\rho$, $u' \equiv q_z\rho'$, and $\beta \equiv \alpha/q_z$ (α see Eq. (2)), and K_0 is the modified Bessel function of the second kind.

References

[1] Pinczuk A, Rink S S and Danan G 1989 *Phys. Rev. Lett.* **63** 1633

[2] Goni A R, Pinczuk A, Weiner J S, Calleja J M, Denni s B S, Pfeiffer L N and West K W 1991 *Phys. Rev. Lett.* **67** 3298

[3] Chen G H, Zhang F Q and Xu X X 1983 *Acta Phys. Sin.* **32** 803 (in Chinese)

[4] Strenz R, Bockelmann U, Hirler F, Abstreiter G, Bohm G and Weimann G 1994 *Phys. Rev. Lett.* **73** 3022

[5] Yang H X, Han R and Wang P 2008 *Chin. Phys.* B **17** 3459

[6] Liu X H, Wang X H and Gu B Y 2001 *Phys. Rev.* B **64** 195322

[7] Kushwaha M S and Sakaki H 2004 *Phys. Rev.* B **69** 155331

[8] Li Q P and Sarma S D 1991 *Phys. Rev.* B **43** 11768

[9] Borges A N, Leao S A and Hipolito O 1997 *Phys. Rev.* B **55** 4680

[10] Ashraf S S Z and Sharma A C 2005 *J. Phys.*: *Condens. Matter* **17** 3043

[11] Wang Y, He X J, Wu Y M, Wu Q, Mei J S, Li L W, Yang F X, Zhao T and Li L W 2011 *Acta Phys. Sin.* **60** 107301 (in Chinese)

[12] Wang L, Cai W, Tan X H, Xiang Y X, Zhang X Z and Xu J J 2011 *Acta Phys. Sin.* **60** 067305 (in Chinese)

[13] Bkshi P, Kempa K, Sqcorupsky A, Du C G, Feng G, Zobl R, Strasser G, Rauch C, Pacher C, Unterrainer K and Gornik E 1999 *Appl. Phys. Lett.* **75** 1685

[14] Atwater H A and Polman A 2010 *Nat. Mater.* **9** 205

[15] Yang X R, XU B, Wang H F, Zhao G Q, Shi S H, Shen X Z, Li J F and Wang Z G 2011 *Chin. Phys. Lett.* **28** 027801

[16] Yao W J, Yu Z Y and Liu Y M 2010 *Chin. Phys.* B **19** 077101

[17] Zhang H, Zhang C Y, Zhang H L and Liu J J 2011 *Acta Phys. Sin.* **60** 077301 (in Chinese)

[18] Bratschitsch R, Muller T, Kersting R, Strasser G and Unterrainer K 2000 *Appl. Phys. Lett.* **76** 3501

[19] Parkinson P, Lloyd H J, Gao Q, Tan H H, Jagadish C, Johnston M B, Herz L M 2007 *Nano. Lett.* **7** 2162

[20] Jung G B, Cho Y J, Myung Y, Kim H S, Seo Y S, Park J and Kang C 2010 *Opt. Express* **18** 16353

[21] Persson M P and Xu H Q 2006 *Phys. Rev.* B **73** 035328

[22] Davydok A, Biermanns A, Pietsch U, Grenzer J, Paetzelt H, Gottschalch V and Bauer J 2009 *Phys. Status Solidi* A **206** 1704

[23] Lee H G, Jeon H C, Kang T W and Kim T W 2001 *Appl. Phys. Lett.* **78** 3319

[24] Kayes B M, Atwater H A and Lewis N S 2005 *J. Appl. Phys.* **97** 114302

[25] Willander M, Nur O, Zhao Q X *et al.* 2009 *Nanotechnology* **20** 332001

[26] Ludeke R and Koma A 1976 *J. Vac. Sci. Technol.* **13** 241

[27] Gregory P E, Spicer W E, Ciraci S and Harrison W A 1974 *Appl. Phys. Lett.* **25** 511
[28] Chruscinski D 2006 *Ann. Phys.* **321** 840
[29] Pinczuk A and Abstreiter G 1989 *Light Scattering in Solids* V (Berlin: Springer Verlag) p. 153
[30] Wendler L and Grigoryan V G 1994 *Phys. Stat. Sol.* (b) **181** 133
[31] Martorell J and Sprung D W 1996 *Phys. Rev.* B **54** 11386
[32] Vazifehshenas T 2008 *Phys. Stat. Sol.* (a) **205** 1302
[33] Matsumodo T, Haraguchi M, Fukui M, Kubo H and Hamaguchi C 1996 *Jpn. J. Appl. Phys.* **35**2068
[34] Shmelev G M, Chaikovskii I A, Pavlovich V V and Epshtein E M 1977 *Phys. Stat. Sol.* (b) **80** 697